Supporting Information

Fe_2NiSe_4/holey-graphene composite with superior rate capability enabled by in-plane holes for sodium-ion batteries

Zixin Wu[a], Xuejie Wang[a], Shenghua Hou[a], Xilong Zhang[a], Xinming Nie[b]*, Jiaguo Yua*, Tao Liu[a]*

a. Laboratory of Solar Fuel, Faculty of Materials Science and Chemistry, China University of Geosciences, 68 Jincheng Street, Wuhan, 430078, P. R. China.

b. School of Physics and Electronic Engineering, Jiangsu Normal University, Xuzhou, Jiangsu 221116, China

*Corresponding author

E-mail: nxinming@jsnu.edu.cn; yujiaguo93@cug.edu.cn; liutao54@cug.edu.cn

Experimental section

Preparation of FNS@HG

FNS@HG was synthesized through a chemical bath deposition method followed by a two-step calcination process. Initially, the prepared GO was dispersed in deionized water. Subsequently, 58.2 mg of $Ni(NO_3)_2 \cdot 6H_2O$ and 161.6 mg of $Fe(NO_3)_3 \cdot 9H_2O$ were dissolved in 30 mL of deionized water and gradually added to a 30 mL GO suspension (5 mg mL^{-1}) with constant stirring. The suspension was subjected to ultrasonication for 30 minutes, followed by continuous stirring at room temperature for 12 hours. After stirring, 0.4 mL of ammonium hydroxide was added. The mixture was then stirred at 80 ℃ for 4 hours and freeze-dried for 24 hours, yielding Fe_2Ni-precursor@rGO. In the second step, the Fe_2Ni@HG nanoparticle composite was obtained by calcination at 800 ℃ under a nitrogen atmosphere for 2 hours. Finally, Fe_2Ni@HG was selenized at 650 ℃ under nitrogen for 2 hours to form FNS@HG. For comparison, FNS@rGO was prepared by directly selenizing Fe_2Ni-precursor@rGO at 650 ℃ under nitrogen for 2 hours.

Preparation of NVP/C

The synthesis of NVP/C was achieved through a facile spray-drying method. Initially, V_2O_5 (20 mmol) was dispersed in deionized water. Oxalic acid (60 mmol) was then added under stirring at 80°C to reduce V^{5+} ions to V^{4+}. Subsequently, NaH_2PO_4 (60 mmol) was gradually introduced with continuous stirring. Finally, 12% sucrose (relative to the theoretical product mass) was added to the mixture and stirred until completely dissolved. The resulting slurry was spray-dried in a nitrogen atmosphere to form a solid $Na_3V_2(PO_4)_3$ precursor. This precursor was then pre-sintered at 350 ℃ for 4 hours, followed by calcination at 800 ℃ for 6 hours in a nitrogen atmosphere, with a heating rate of 5 ℃ min^{-1}, resulting in the formation of NVP/C.

Material characterization

The crystal structures of all materials were confirmed using a powder X-ray diffractometer (XRD, LabX XRD-6100). Electrochemical in-situ XRD tests were

conducted to reveal structural changes during the electrochemical process. The morphology of the synthesized materials was examined using a field emission scanning electron microscope (FE-SEM, Regulus 8100). High-resolution transmission electron microscopy (HRTEM) images and energy-dispersive spectroscopy (EDS) mappings were obtained using a FEI TECNAI G2 F20 instrument. X-ray photoelectron spectroscopy (XPS) patterns were collected using an ESCALab 250Xi electron spectrometer.

Electrochemical Measurements

All sodium-ion half and full cells were assembled in CR2032-type coin cells within an argon-filled glovebox (H_2O < 0.1 ppm, O_2 < 0.3 ppm). Electrodes were prepared by mixing 70 wt% active material, 20 wt% conductive carbon black, and 10 wt% polyvinylidene difluoride (PVDF) binder in N-methyl-2-pyrrolidone (NMP). The resulting slurry was coated onto copper foil and dried in a vacuum oven at 60°C for 10 hours. The loading mass of the active material was approximately 2.5 mg cm^{-2}. The electrolyte was a solution of 1 M $NaPF_6$ in 1,2-dimethoxyethane (DME), and glass fiber was used as the separator. Galvanostatic discharge/charge (GCD) measurements were performed using a Neware system to evaluate the electrochemical properties of the electrodes. Cyclic voltammetry (CV) curves were acquired with a Versa STAT 3 electrochemical station within the voltage range of 0.01 to 3.00 V. Electrochemical impedance spectroscopy (EIS) measurements were performed over a frequency range from 100,000 Hz to 0.1 Hz with a signal amplitude of 5.0 mV. The galvanostatic intermittent titration technique (GITT) involved cycling the cells at 0.1 C for 30 minutes, followed by a 5-hour relaxation period. The Fe_2NiSe_4@HG anode was assembled into sodium-ion full cells using $Na_3V_2(PO_4)_3$ as the cathode. The mass loading ratio of the negative and positive electrodes was approximately 4.45. The N/P ratio of FNS@HG||NVP was about 1.12.

This manuscript uses a formula to calculate Na^+ diffusion coefficient：

$$D_{Na^+} = \frac{4}{\pi\tau}\left(\frac{m_B V_M}{M_B S}\right)^2 \left(\frac{\Delta E_s}{\Delta E_t}\right)^2 \qquad (1)$$

In this formula, τ is the relaxation time, m_B and M_B are the mass and relative molecular mass of the electrode material, respectively. ΔE_s and ΔE_t are the change in steady state voltage values before and after the titration and the change in voltage during the titration process, respectively. S is the contact area of the electrode with the electrolyte (cm^{-2})

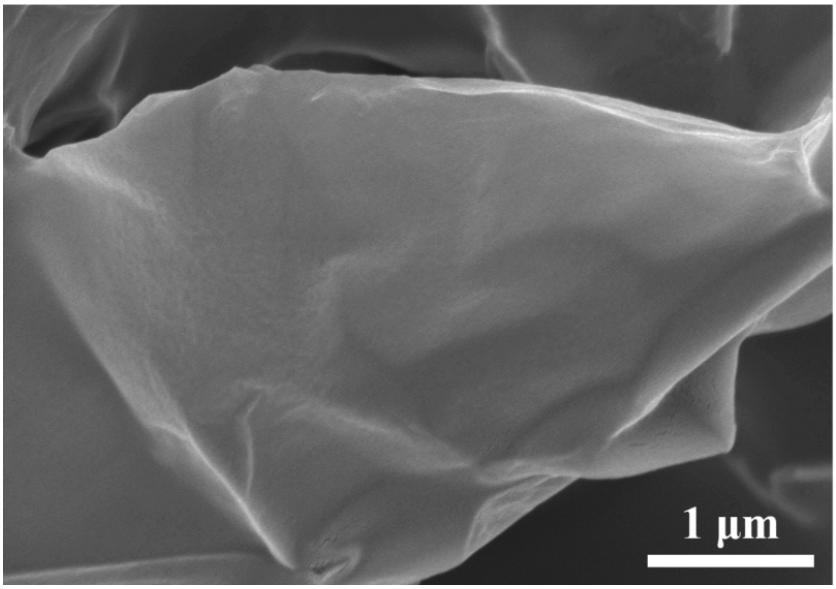

Figure S1. FE-SEM image of GO

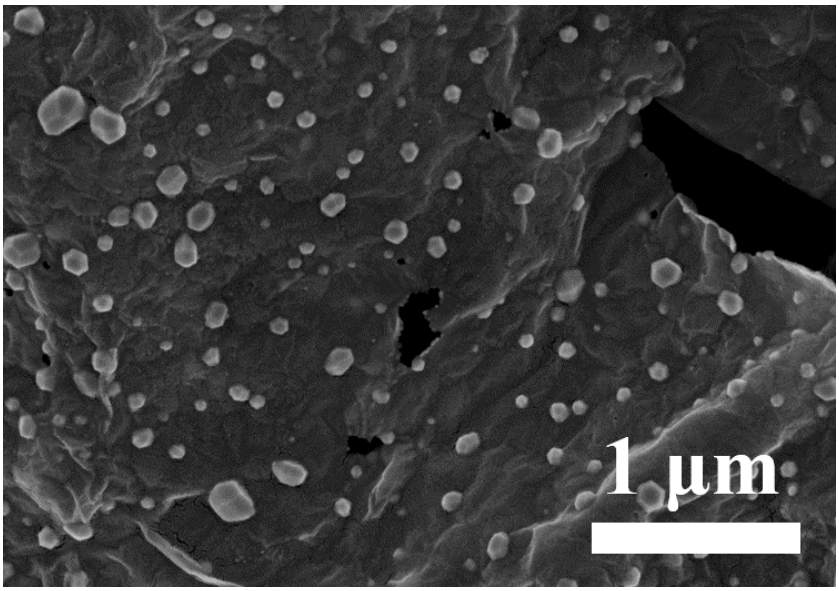

Figure S2. FE-SEM image of FNS@rGO.

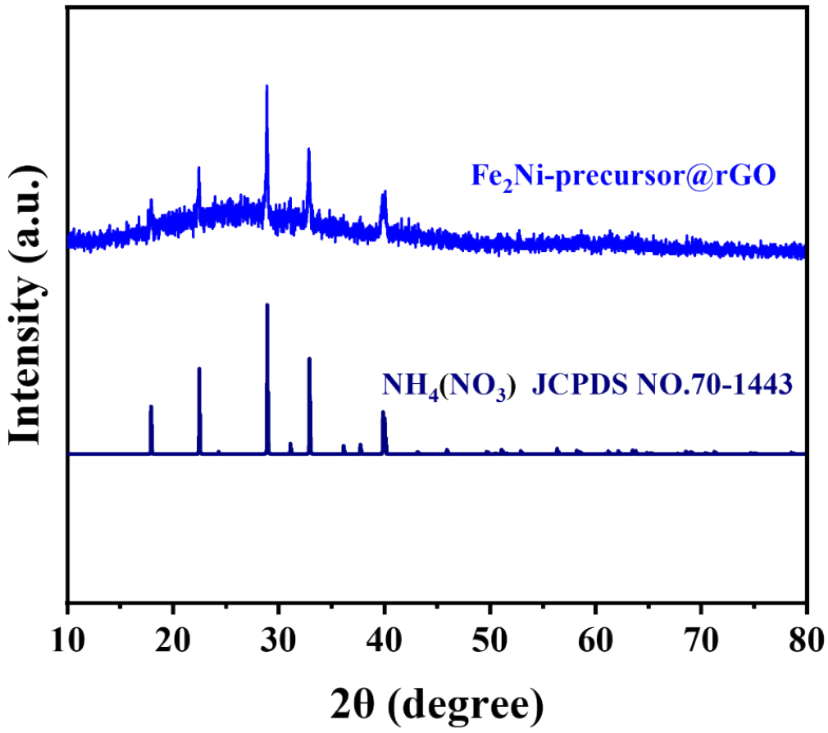

Figure S3. XRD pattern of Fe_2Ni-precursor.

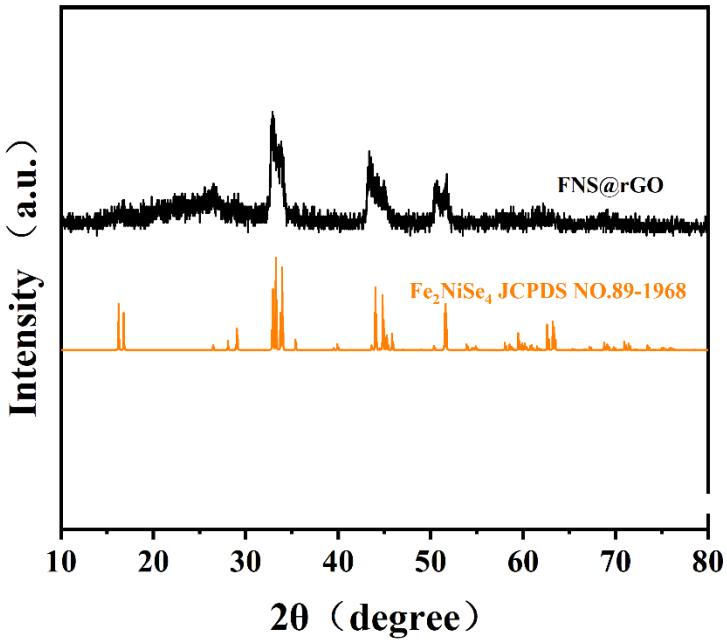

Figure S4. XRD pattern of FNS@rGO.

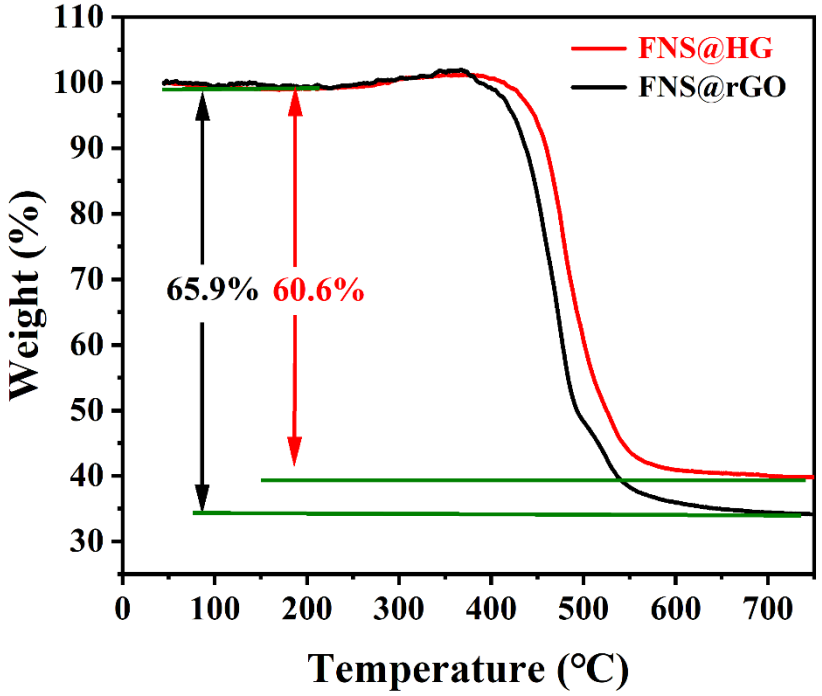

Figure S5. TGA profiles of FNS@HG and FNS@rGO.

The calculated procedure for carbon content from TGA:

m_g	Fe_2O_3	NiO
FNS@HG	1.024*[159.7/ (159.7+74.7)] =0.698 mg	1.024*[74.7/ (159.7+74.7)] =0.326 mg
FNS@rGO	0.968*[159.7/ (159.7+74.7)] =0.66 mg	0.968*[74.7/ (159.7+74.7)] =0.308 mg

$Fe_2NiSe_4 + 6O_2 \rightarrow Fe_2O_3 + NiO + 4SeO_2\uparrow$

486.24 g/mol 159.7 g/mol 80.02 g/mol

FNS@HG: 2.125 mg 0.698 mg 0.326 mg

FNS@rGO: 2.01 mg 0.66 mg 0.308 mg

$m_{g(HG)} = m_{g(FNS@HG)} - m_{g(FNS)} = 2.598 - 2.125 = 0.473$ mg $C_{wt\%} = 0.473/2.598 = 18.2\%$

$m_{g(rGO)} = m_{g(FNS@rGO)} - m_{g(FNS)} = 2.838 - 2.01 = 0.828$ mg $C_{wt\%} = 0.828/2.838 = 29.2\%$

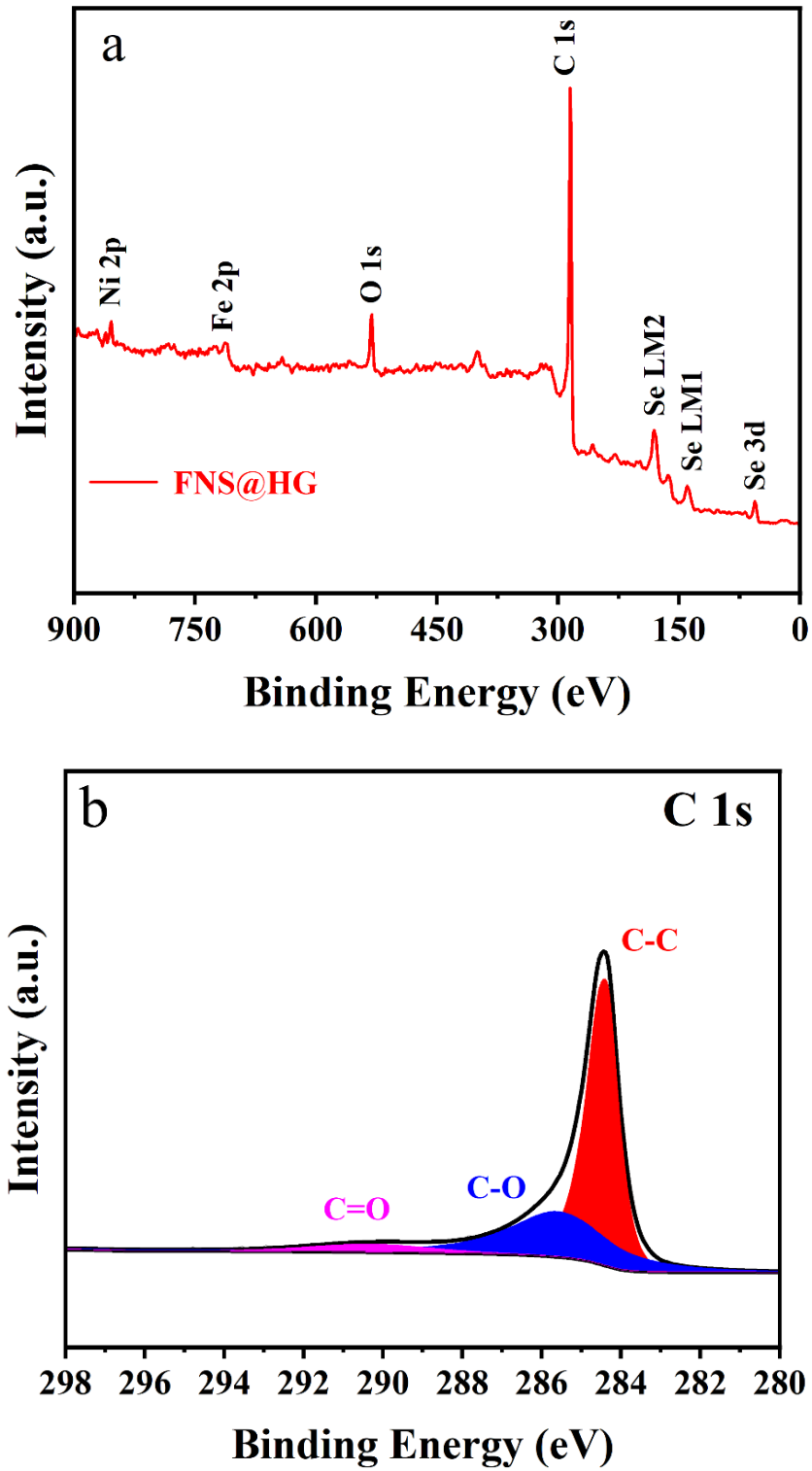

Figure S6. (a) Survey spectrum, (b) high-resolution spectrum of C 1s of FNS@HG and FNS@rGO

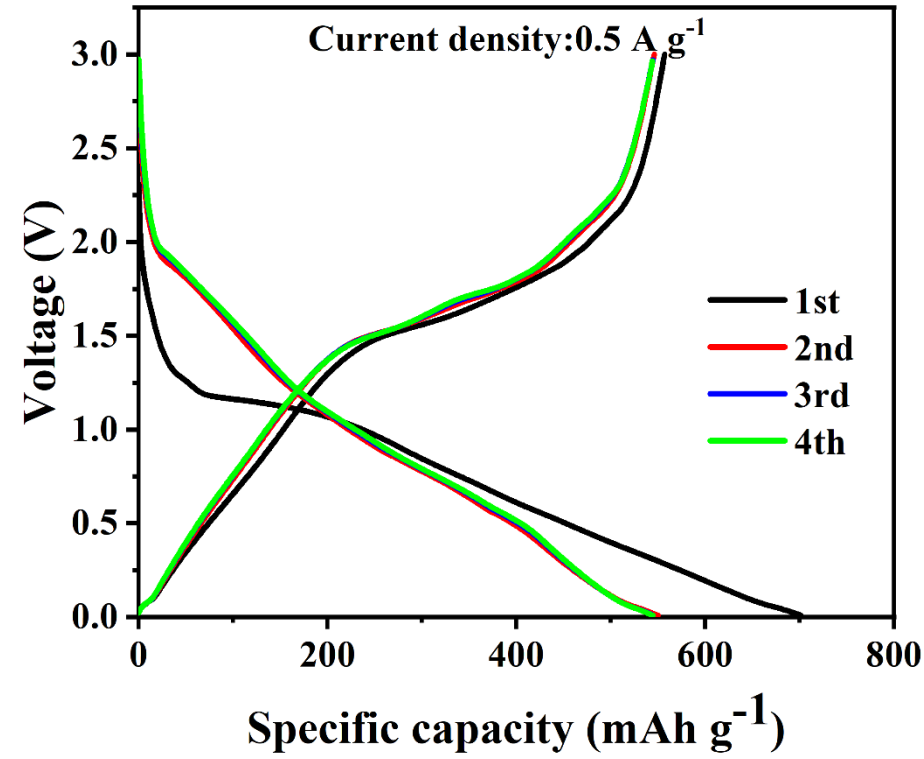

Figure S7. GCD curves of FNS@HG.

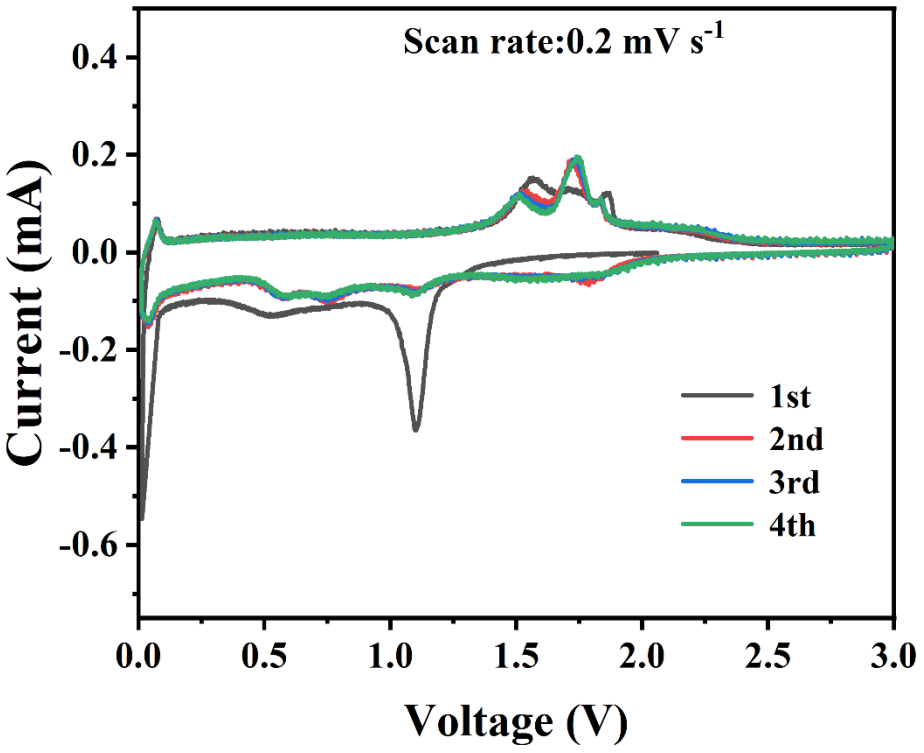

Fig. S8 CV curves of FNS@HG at 0.2 mV s^{-1}.

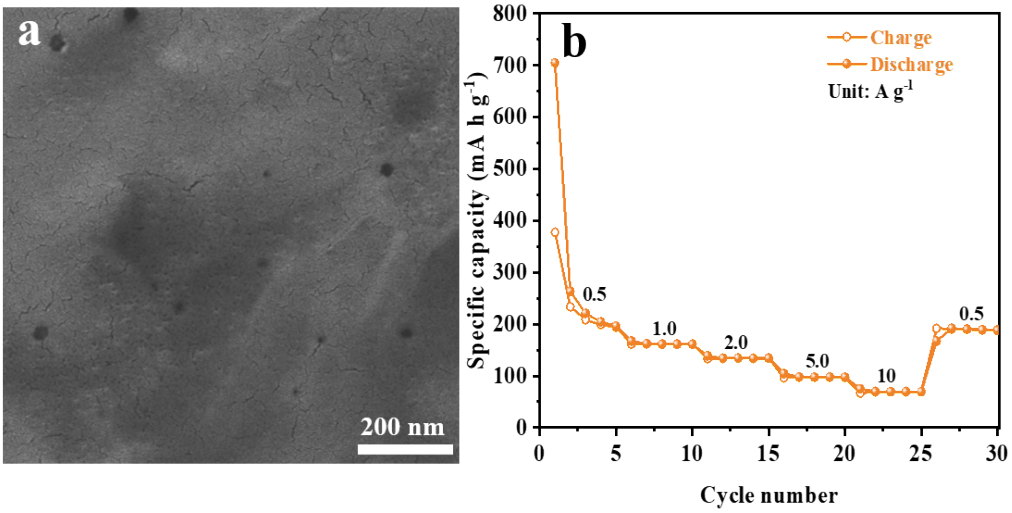

Fig. S9 (a) FE-SEM image and (b) rate performance of HG.

HG displayed specific capacities of 377.4, 201, 161.7, 133.4, 96.2 and 66.8 mA h g^{-1} at 0.1, 0.5, 1, 2, 5, and 10 A g^{-1}, respectively (Fig.S14). According to the content of HG in FNS@HG, the capacity contributions of HG in FNS@HG were 36.6, 29.4, 24.3, 17.5 and 12.2 mA h g^{-1} at 0.5, 1, 2, 5, and 10 A g^{-1}, respectively, indicating that HG contributed less to the total capacity of FNS@HG.

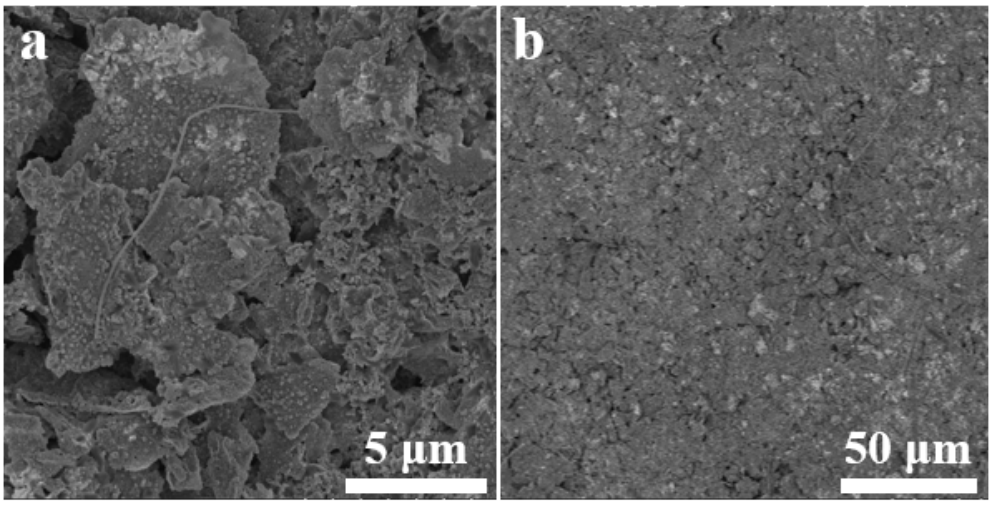

Fig. S10 FE-SEM images of cycled FNS@HG anode

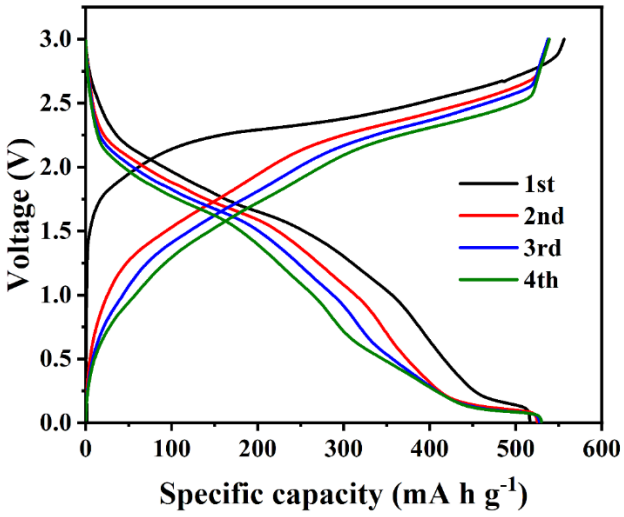

Fig. S11. GCD curves of FNS@HG||NVP

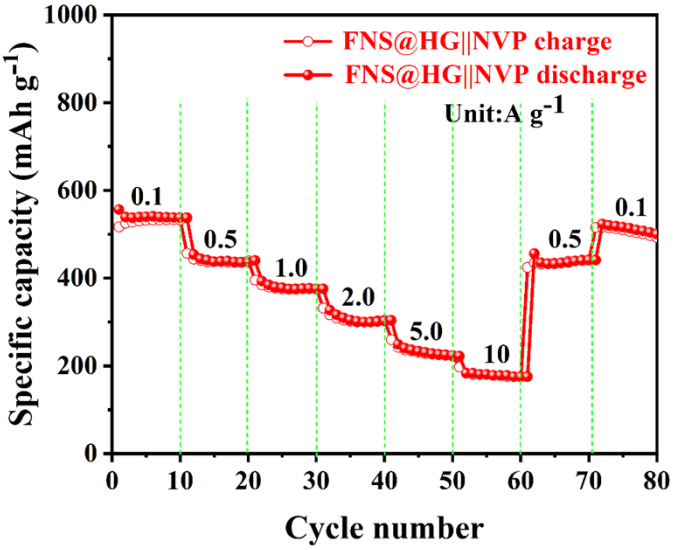

Fig. S12 Rate performance of FNS@HG||NVP

$Na_3V_2(PO4)_3$/C (NVP) was used as a cathode and FNS@HG electrode was assembled into a complete cell to further evaluate its electrochemical performance. The GCD test (Fig. S11) was performed in the voltage range of 0.01~3 V, and the specific capacity of the full cell was calculated using the mass of FNS@HG anode. As shown in Fig. S12, FNS@HG||NVP displayed a reversible capacity of 556.22, 453.53, 392.97, 326.18 and 248.74 mA h g^{-1} at 0.1, 0.5, 1, 2, 5, and 10 A g^{-1}, respectively. The reversible capacity of 523.53 mA h g^{-1} was still demonstrated when the cell returned

from10 A g^{-1} to 0.1 A g^{-1}, indicating that the cell had excellent reversibility. The reversible capacity of 523.5 mA h g^{-1} was still demonstrated when the cell returned to 0.1 A g^{-1}, indicating that the cell had excellent reversibility. This detailed electrochemical analysis highlights the enhanced rate performance, cycling stability, and Na^+ storage mechanism of FNS@HG, confirming its potential as a high-performance anode material for sodium-ion batteries. This detailed electrochemical analysis highlights the enhanced rate performance, cycling stability, and Na^+ storage mechanism of FNS@HG, confirming its potential as a high-performance anode material for sodium-ion batteries.

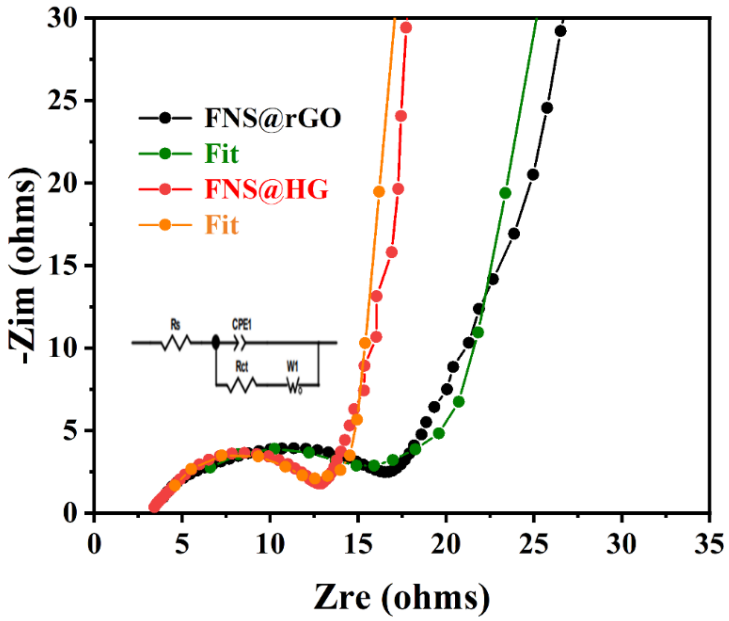

Fig. S13 Nyquist plots of FNS@HG and FNS@rGO

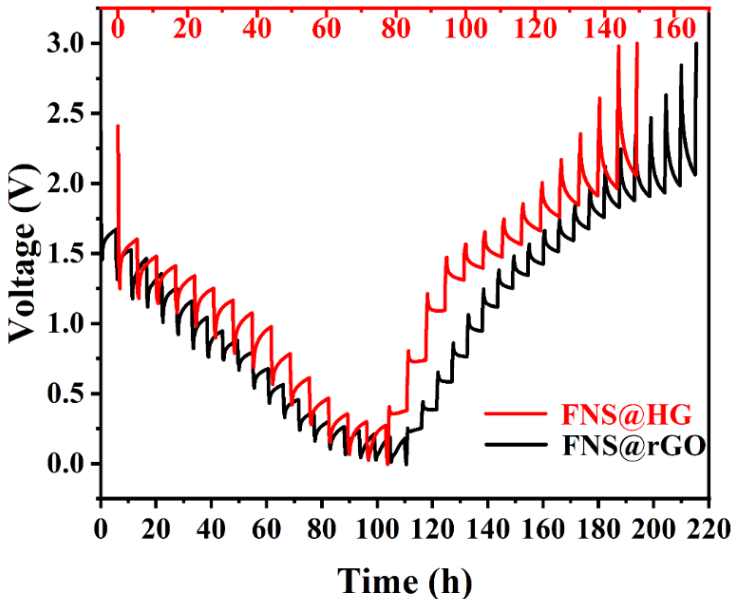

Figure S14. GITT profiles of FNS@HG and FNS@rGO.